2-1-2016

Design of a Multi-Pinhole Collimator for I-123 DaTscan Imaging on Dual-Headed SPECT Systems in Combination with a Fan-Beam Collimator

Michael A. King
University of Massachusetts System

Joyeeta M. Mukherjee
University of Massachusetts System

Arda Könik
University of Massachusetts System

I. George Zubal
Z-Concepts LLC

Joyoni Dey
Louisiana State University

See next page for additional authors

Recommended Citation

King, M., Mukherjee, J., Könik, A., Zubal, I., Dey, J., & Licho, R. (2016). Design of a Multi-Pinhole Collimator for I-123 DaTscan Imaging on Dual-Headed SPECT Systems in Combination with a Fan-Beam Collimator. *IEEE Transactions on Nuclear Science, 63* (1), 90-97. https://doi.org/10.1109/TNS.2016.2515519

Published in final edited form as:

IEEE Trans Nucl Sci. 2016 February ; 63(1): 90–97. doi:10.1109/TNS.2016.2515519.

Design of a Multi-Pinhole Collimator for I-123 DaTscan Imaging on Dual-Headed SPECT Systems in Combination with a Fan-Beam Collimator

Michael A. King [Senior Member IEEE],
Department of Radiology, University of Massachusetts Medical School Worcester, MA 01655 USA

Joyeeta M Mukherjee [Senior Member IEEE],
Department of Radiology, University of Massachusetts Medical School Worcester, MA 01655 USA

Arda Könik [Associate Member, IEEE],
Department of Radiology, University of Massachusetts Medical School Worcester, MA 01655 USA

I. George Zubal [Member IEEE],
Z-Concepts, L.L.C., New Haven, CT

Joyoni Dey [Member IEEE], and
Department of Physics & Astronomy, Louisiana State University, LA

Robert Licho
Department of Radiology, UMassMemorial Healthcare, Worcester, MA 01655 USA

Michael A. King: Michael.King@umassmed.edu

Abstract

For the 2011 FDA approved Parkinson's Disease (PD) SPECT imaging agent I-123 labeled DaTscan, the volume of interest (VOI) is the interior portion of the brain. However imaging of the occipital lobe is also required with PD for calculation of the striatal binding ratio (SBR), a parameter of significance in early diagnosis, differentiation of PD from other disorders with similar clinical presentations, and monitoring progression. Thus we propose the usage of a combination of a multi-pinhole (MPH) collimator on one head of the SPECT system and a fan-beam on the other. The MPH would be designed to provide high resolution and sensitivity for imaging of the interior portion of the brain. The fan-beam collimator would provide lower resolution but complete sampling of the brain addressing data sufficiency and allowing a volume-of-interest to be defined over the occipital lobe for calculation of SBR's. Herein we focus on the design of the MPH component of the combined system. Combined reconstruction will be addressed in a subsequent publication. An analysis of 46 clinical DaTscan studies was performed to provide information to define the VOI, and design of a MPH collimator to image this VOI. The system spatial resolution for the MPH was set to 4.7 mm, which is comparable to that of clinical PET systems, and significantly smaller than that of fan-beam collimators employed in SPECT. With this set, we compared system sensitivities for three aperture array designs, and selected the 3 × 3 array due to it being the highest of the three. The combined sensitivity of the apertures for it

was similar to that of an ultra-high resolution fan-beam (LEUHRF) collimator, but smaller than that of a high-resolution fan-beam collimator (LEHRF). On the basis of these results we propose the further exploration of this design through simulations, and the development of combined MPH and fan-beam reconstruction.

I. Introduction

The 2011 FDA approval of the SPECT imaging agent I-123 labeled DaTscan (ioflupane) for diagnosis and monitoring progression of Parkinson's Disease (PD) [1], has opened up a new era in SPECT brain imaging . Unlike with perfusion imaging where the entire brain is the volume of interest (VOI), with PD the structures of interest are the putamen, caudate and potentially substantia nigra, which lie in the central interior portion of the brain (Fig 1A). However, imaging of the occipital lobe is also required with PD for calculation of the striatal binding ratios (SBR) which is/are calculated as [(counts per minute (cpm) /voxel in putamen(s) and/or caudate(s)) – (cpm/voxel in occipital lobe)] / (cpm/voxel in occipital lobe). The SBR is a parameter of significance in the early diagnosis, differentiation of PD from other disorders with similar clinical presentations, and monitoring progression [2–6]. Fig 1B shows the current state of clinical imaging where the putamen and caudate are not separated in the reconstructed slices leading to difficulties in the independent calculation of the caudate's or putamen's binding ratio.

As illustrated by the GE Alcyone multi-pinhole (MPH) clinical-SPECT system [7], a dramatic gain in combined resolution / sensitivity can be obtained through imaging with specially designed SPECT systems with multiple tailored pinhole collimators focused on viewing the heart. Thus the proposal to design and construct such a system dedicated to SPECT brain imaging would be a natural choice [8–14]. However, the excessive cost of these systems, particularly for imaging procedures utilized less commonly than cardiac perfusion imaging, is likely prohibitive. Thus we believe the time is right for disease-specific MPH collimator designs with coupled iterative reconstruction to be employed with existing, widely available, clinical SPECT systems. The MPH collimator would be designed to provide enhanced spatial resolution / sensitivity for the interior of the brain. The fan-beam collimator would provide lower resolution but complete sampling of the brain addressing data sufficiency and allowing a volume-of-interest to be defined over the occipital lobe for calculation of SBR's. Combined iterative reconstruction of the images from the two collimators would be employed to provide the slices.

In this paper we focus on the design of the MPH component of the combined system. Combined reconstruction will be addressed in a subsequent publication.

II. Fan-Beam Component of Combined Imaging

Instead of designing a fan-beam collimator specifically for combined imaging we decided to employ a low-energy ultra-high-resolution (LEUHR) design, which has been used very successfully for brain imaging since the mid 1990's with the Picker Prism3000 three-headed SPECT system. This collimator has a 50 cm focal length, a 1.40 mm hole size, a 34.9 mm hole length, and a 0.15 mm septal thickness.

III. Design Constraints for MPH Brain Imaging

In designing the MPH we chose to achieve a system spatial resolution ($FWHM_S$) of 4.7 mm at the focal point of the apertures. This resolution was selected as it is in the range of the resolution of current whole-body PET systems [15], which can differentiate the caudate from the putamen and conventional SPECT currently cannot. It also resulted in sensitivity at this location for a 3 × 3 array of apertures equal to that of LEUHR fan-beam collimators employed clinically.

The Philips BrightView (BV) XCT is the clinical SPECT system we chose for initial testing of this approach once developed and an MPH collimator is fabricated. Thus our design was centered on clinical application of this system. The BV has detector heads with an imaging field-of- view (FOV) of 54 cm laterally and 40.6 cm axially. We have observed during the past more than 20 years usage of the Picker (now Philips) Prism3000 three-headed SPECT system for brain imaging in our department, that a distance of 13.0 cm or less from the axis-of rotation (AOR) to collimator face is employed as the radius-of-rotation (ROR) in clinical imaging. Preliminary observations indicate this is also true on our BV system when imaging with the head holder from Philips. Thus we designed our MPH for a 13.5 cm ROR from the AOR to the center of the face of aperture plate, with the extra 0.5 cm as an added safety margin. With the aperture 0.5 cm deep on the side towards the patient this results in a distance of 14.0 cm from the AOR to the aperture.

With the ROR established, we next determined the centering and extent of the volume-of-interest (VOI) to be imaged by our MPH system. In rotating the camera heads about a patient it is necessary to clear the patient's shoulders. One can do this by centering the patient's head axially in the FOV, and then using a large ROR to keep the collimators from contacting the patient. However, this large ROR would cause an undue loss of spatial resolution and sensitivity because of their strong distance dependence for pinhole collimators [16]. To achieve the ROR of 13 cm or less which we determined is being employed clinically on our Prism3000, the patient was moved into the imaging volume axially just to an extent such that the camera heads stayed superior to the patients' shoulders during acquisition. Thus the patients' heads were not centered axially relative to the detector, but instead displaced caudally. Note that once patients have been moved superiorly in the imaging volume to the maximum extent allowable for the camera-heads to continue to clear their shoulders, they can be moved in no further. Thus our task was to determine the likely minimum distance between the center of the striatal region we wish to image and the superior extent of the shoulders in a patient population. This was then used for specifying the axial level relative to the detector where the central axes of all the pinholes were to be focused. This "focal point" of the pinholes was also the center of our design VOI. The minimum distance was of interest as under p-scope guidance patients with a greater distance between the center of their striatal region and shoulders can be moved out inferiorly to center their striatum at the focal point.

The patient population we employed for the task of defining the VOI was 46 de-identified existent I-123 DaTscan studies acquired on Prism3000 SPECT systems downloaded from the Parkinson's Progressive Markers Initiative (PPMI) web site [http://www.ppmi-info.org/

data] (for up-to-date information on PPMI, visit www.ppmi-info.org). Based on the expectation that PD occurs with a likelihood of 1.5–1.9 times greater in men than women [17, 18], there were most likely proportionately more males than females in this study population. We are unable to definitively provide the demographics of our population as in the process of de-identification patient gender was hidden from us. Only 4% of patients present with PD before an age of 50 [18]. Thus it is not a disease of childhood and we therefore do not expect usage of combined imaging with children. The size of our population was based on that available to us at the time we performed this analysis, and was not selected on a statistical basis. Thus we can provide no statistical justification that this population is of an appropriate size to base our analysis upon.

The patient acquisitions were reconstructed with our OSEM fan-beam reconstruction code with attenuation correction and resolution recovery followed by 3D post-reconstruction Gaussian smoothing [19]. We generated two images from these slices for each patient for use in setting constraints on the design of our MPH system. The first was to do a parallel reprojection of the slices to remove the lateral distortion caused by fan-beam imaging. This was performed at each of the 120 acquisition angles the studies were acquired over 360°. These reprojections were then summed to provide an image, which portrayed the distribution of DaTscan in the head as seen in the projection images (minus the impact of attenuation) when averaged over all viewing angles. These images were displayed and the axial centers of the striatal distribution of DaTscan were indicated interactively as illustrated in Figure 2A. From these axial centers the offsets to the known location of the caudal edge of the detector FOV were determined. For the 46 patient studies in our population we determined the offsets ranged from 6.1–10.7 cm, with a mean ±SD of 7.9±1.2. We therefore selected a 6.0 cm axial offset from the caudal edge of the detector for the location of the focal point of the pinholes. Similarly, as illustrated in Figure 2A we interactively determined the axial extent of the striatal region about this center point. For the 46 patient studies in our population the extent ranged from 2.8–5.0 cm, with a mean ±SD of 3.8±0.6 cm. To allow for some degree of variability in patient positioning and still encompass the striata and substantia nigra we chose to image the volume of 4 cm to either side of the focal point, for an 8 cm total axial extent of our target VOI.

Brain reach is the axial distance between the side-shielding of the camera head and caudal edge of the imaging volume. Thus it is the minimum axial extent of a patient’s anatomy lost in brain imaging superior to the patient’s shoulders, when the camera head just clears the shoulders during acquisition. When designing MPH collimators for brain imaging on different SPECT systems, any difference in brain reach should be taken into consideration in determining the axial location of the pinhole focal point for striatal imaging. Since the brain reach of the Prism3000 (7.5 cm by our measurement) and BrightView (7.4 cm according to the Philips Healthcare 2009 BrightView XCT Technical Specification Pamphlet) are equal we were able to use the Prism3000 studies to determine the location of the focal point of the pinholes on the BrightView.

With the axial center and total height (axial extent) of the VOI for imaging defined as per above, there remained the task of determining the lateral extent of the VOI. To do this we employed the second image generated for each of the DaTscan studies. To form this image

we first summed all the transverse slices of the study. We then the summed the results of rotating this image in 3° steps over 360° about the AOR, as per acquisition. The summed image thus represented the radial variation in activity. As illustrated in Figure 2B, the lateral extent of the striatal region for each of the 46 patients was determined interactively by having an observer mark the two sides of the striatal region. The result was the lateral extent in the striatal region was observed to range from 6.8–10.0 cm, with a mean ±SD of 8.4±0.9 cm. We allowed a 1 cm margin on each side of the observed maximal in the striatal region and set the width of our VOI to be 12.0 cm in diameter.

Thus our VOI to be imaged by our MPH system was determined to be a cylindrical volume of 8.0 cm in height and 12.0 cm in diameter. Figure 2C illustrates how well this VOI encompasses the striatal region of an example patient in projections, and Figure 2D illustrates that this VOI provides a margin around the edges of the striatal region transversely in all directions.

Our final design constraint was to not allow overlap of the FOV of the apertures on the detector, or multiplexing. This constraint will be reconsidered in future studies based upon the investigations of others [20–23]. We have adopted a novel combined usage of loftholes (rectangular entrance and exit ports)[24, 25] with square apertures[26, 27] for higher sensitivity, lower penetration, and better detector surface area utilization.

III. Multi-Pinhole Designs

With the ROR and VOI design constraints established as discussed in the previous section we designed MPH collimators for arrays of 2 × 2, 3 × 3, and 4 × 4 apertures as shown in Figure 3. In each case we varied the distance between the apertures and detectors until the detector area was filled to the maximum extent possible without overlap of detector irradiation (multiplexing) by two different apertures and minimal truncation of the target VOI was present. Figure 4 shows the resulting layout of the 3 × 3 array of apertures and their FOV's relative to our target VOI as seen in 4A looking along the axial direction with camera heads at rotations of 0 and 180 degrees (side view) and in 4B looking down from above with the two camera heads at rotations of 90 and 270 degrees (top view). The size of the schematic outlines of the head (ellipsoid with axes of 16.1 cm in width, 23.2 cm in depth, and 24.7 cm in height) and shoulders (53.5 cm across) shown in this figure were set to be those of the 95 percentile value dimensions obtained from a technical report on human engineering design data [28]. In this way, we determined the placement of the apertures, distance between them and the detectors (a), and the distance between each aperture and the focal point of the apertures at the center of the VOI (b).

With the magnification (M) determined as the ratio of a/b, for the three arrays of apertures we determined the size of each aperture (d) required to yield a system resolution of 4.7 mm for the 159 keV primary photons of I-123 [29] as imaged by a tungsten-composite [30] square-shaped aperture [31] by

$$d=[(FWHM_S{}^2-(FWHM_I/M)^2)/(1+1/M)^2]^{1/2}. \quad \text{(Eq 1)}$$

In this equation $FWHM_I$ is the intrinsic resolution, which we took as 3.1 mm (listed as typical value in Philips Healthcare 2009 BrightView XCT Technical Specification Pamphlet).

Once the diameter of each aperture was determined we calculated the geometric sensitivity (g) for a I-123 point source as imaged with a square aperture on-axis by [26, 27, 29]

$$g=[d^2/(4\pi b^2)]. \quad \text{(Eq 2)}$$

for each aperture in the array, and then summed them to determine the total geometric efficiency at the focal point of the array on the AOR. We calculated sensitivity for I-123 in cpm/μCi based on a 0.833 abundance for the 159 keV primary photon [30], and a 0.80 photopeak detection efficiency for NaI(Tl) [31].

As shown in Table I, in comparing the three arrays we determined that the 3 × 3 pinhole configuration provided the highest geometric sensitivity. This is because the larger d of the 2 × 2 array did not compensate for only 4 holes being employed as opposed to 9 for the 3 × 3 array. The 4 × 4 array resulted in a decrease in size of the d to reach a $FWHM_S$ of 4.7 mm which caused a larger reduction in sensitivity than could be compensated for by the increased number of pinholes due to the 3.1 mm intrinsic resolution of the detector.

A comparison to the standard collimators used in SPECT imaging to the 3 × 3 MPH is shown in Table II. There resolution and sensitivity were calculated using the equations of Moyer [16] for a point at 13.5 cm along the central axis from face of low-energy high-resolution (LEHR) fan-beam, low-energy ultra-high-resolution (LEUHR) fan-beam, LEHR parallel-hole, and LEUHR parallel-hole collimators for the Philips Prism3000 three-headed SPECT camera, which has been a mainstay of brain imaging for many years. Note the large improvement in spatial resolution of the MPH compared to all the fan-beam and parallel-hole collimators. At the focal point, the MPH is higher in sensitivity than the LEUHR parallel-hole collimator, while matching that of the LEUHR fan-beam collimator. Both LEHR collimators have greater sensitivity than MPH, the LEHR fan-beam collimator by approximately 60%.

For the 3 × 3 pinhole configuration we also investigated how the resolution ($FWHM_S$) and sensitivity vary with radial displacements from the center of the VOI of 2 cm, 4 cm, and 6 cm (one third, two thirds, and the outer edge of the VOI) at mid-level axially. The $FWHM_S$ were calculated by rearranging Eq 1 as

$$FWHM_S=[(d[1+(1/M)])^2+(FWHM_I/M)^2]^{1/2} \quad \text{(Eq 3)}$$

where M now changed as a function the distance between the aperture and source. Note that the values for resolution and sensitivity are for the MPH only, derived from planar projection equations (not image reconstructions), and are not combined in any way with fan beam data. The variation in these with projection angle is shown in Figure 5, and the values averaged over 360 degree rotation are given in Table III. As can be seen from Table III, the large

variations with rotation shown in Figure 5 are averaged out such that there is very little change in resolution and only a modest change in sensitivity. The radial variation in resolution with projection angle means an anisotropic system response of increasing variation will be seen in reconstructions as one moves away from the center of the VOI. This will likely be able to be diminished by including modeling of system response in reconstruction [32].

IV. Discussion

The MPH design provides a spatial resolution at the focal point of the apertures approximately equivalent to that of the current whole body PET systems. This should provide a significant improvement in separation of the caudate and putamen, and improved visualization of the substantia nigra compared with current LEHR and LEUHR fan and parallel collimators employed for clinical brain imaging, at a small cost of that for a dedicated brain-imaging system. The sensitivity is lower than that of the LEHR fan-beam collimator but equivalent to that of the LEUHR fan-beam collimators. In future work we will investigate if the judicious use of multiplexing can be used to significantly further improve sensitivity for the MPH while maintaining spatial resolution and not producing artifacts [20–23].

A numbers of investigations have been performed since the early days of SPECT on improving the collimation employed with gamma-camera based brain imaging including systems with longer bores to bring the end of the collimator closer to the patients head and yet clear the shoulders [32, 33], usage of fan-beam collimation [34, 35], employing half-cone-beam collimators [36], using a combination of converging collimators [37], and by the use of a MPH collimator [31]. The preceding MPH collimator [31] was for application to DaTscan imaging, as is our proposed MPH. The authors set the distance between the 7.5 mm diameter aperture and the AOR to 19.3 cm to allow the aperture plate to go around the shoulders and designed the system for a significant (over an order of magnitude) increase in sensitivity over conventional parallel-hole collimators. This resulted in a spatial resolution of 2.06 cm FWHM at a distance of 10 cm from the face of their aperture plate, and a sensitivity of 2,366 cpm/μCi. Note that both of these values would degrade significantly at the center of the brain, which is 19.3 cm from the aperture plate.

Our design goal was to improve spatial resolution while approximately maintaining sensitivity. This is because spatial resolution has a very significant impact on the apparent contrast of structures whose smallest dimension is less than 2–3 times the FWHM of the imaging system [33, 34]. It also impacts the ability to separate two structures which are close to each other as illustrated in Fig 1B for the caudate and putamen. Muehllehner [35] has shown that image contrast improved rapidly with spatial resolution improvements for high contrast structures like in DaTscan imaging such that “significantly fewer counts are needed to give images of comparative visual quality”. Also Mueller, et al [36], showed for brain SPECT imaging “collimators designed for high resolution, even at substantial cost in sensitivity, are expected to yield significant improvements”. Thus we have chosen to optimize for improved spatial resolution by having our system move close to image the patient with the camera-head positioned superior to the shoulders, instead of circling around

the shoulders, and using a 2.2 mm square as opposed to 7.5 mm round aperture. However, it is possible that one may be able to obtain PET like spatial resolution in brain SPECT and not give up as much in sensitivity. Van Audenhaege et al. [14] in simulations determined that by usage of resolution modeling in iterative reconstruction they were able to visualize 4 mm hot-rods when their target resolution was 6 mm at the center of their FOV. Thus it may be that larger apertures than those we determined herein can be employed which would result in improved sensitivity. To answer this question we plan to perform a task-based study of aperture size for lesion detection and quantification in DaTscan imaging before we fabricate and test an actual MPH collimator for combined reconstruction.

Another collimation design for brain SPECT which is close to ours is the combination of a 40 cm focal length fan-beam collimator on one head with a 20 cm focal length cone-beam collimator whose focal point is shifted inferiorly on the second head of dual-headed SPECT systems [37]. This innovative system was also designed to provide improved sensitivity within the central region of the brain. As shown in their figures with a 15 cm radius-of-rotation, the 20 cm focal length cone-beam collimator provides very large gains in sensitivity compared to a parallel-hole collimator in a region around the AOR. Using the collimator specifications given in their paper and the collimator equations in Moyer [16], we determined this system would yield a system resolution at the AOR which is approximately a factor of 1.5 larger than the calculated resolution of our system. The sensitivity was estimated to be > 6 times that of our MPH design.

In this paper we have detailed the analysis that went into our design for a MPH collimator for combined usage with a fan-beam collimator for I-123 DaTscan imaging. We have left discussion of the iterative reconstruction of the projection data from these two different types of collimators to a paper on that topic. There we will address the question of to what extent we will be able to maintain the best characteristics of the MPH collimator within our VOI and seamlessly transition to having the region beyond our VOI preserving the features of fan-beam imaging. We have also not considered septal penetration in this paper, even for the 159 keV primary photons of I-123. For these penetration will increase sensitivity at the expense of increasing the measured $FWHM_S$ (lowering spatial resolution) [38]. Thus the sensitivity and resolution of an actual MPH collimator will differ from those given herein. For I-123 the presence of the low-abundance photons higher in energy than the primary photons [30] will further complicate experimental sensitivity and resolution measurements.

V. Conclusion

By analyzing 46 DaTscan clinical studies, we determined the VOI of interest for MPH imaging of DaTscan to be a cylindrical volume 12.0 cm in diameter and 8.0 cm in height centered axially 6.0 cm from the caudal edge of the camera detector with a 7.4 cm brain reach. We then investigated three different arrays of apertures, and subject to the constraints present in this paper determined a 3 × 3 aperture array to provide better sensitivity than 2 × 2 or 4 × 4 arrays designed to have the same system spatial resolution at the center of the VOI. This design provided striatal imaging with equivalent sensitivity at the center of the VOI as a LEUHR-fan beam collimator used for brain imaging and substantially better spatial resolution (4.7 mm versus 7.4 mm) at this location. On the basis of these results we propose

the exploration of further improvements in design especially a task-based study of the aperture size, and the development of combined MPH and fan-beam reconstruction for high spatial resolution imaging of the striatal region of the brain with I-123 DaTscan SPECT imaging.

Acknowledgments

The authors would like to thank the reviewers and associate editor for their many excellent comments with significantly improved this manuscript. An early version of these investigations were presented at the 2012 IEEE Nuclear Science Symposium and Medical Imaging Conference and published in its proceedings as King MA, Zubal IG, Mukherjee JM, Konik A, Dey J, Licho R. Design of a combined fan and multi-pinhole collimator combination for clinical I-123 DaTscan imaging on dual-headed SPECT systems. Proceedings of 2012 IEEE Nuclear Science Symposium and Medical Imaging Conference, MIC16-34, pp 3170-3173, 2012. Data used in the preparation of this article were obtained from the Parkinson's Progression Markers Initiative (PPMI) database (www.ppmi-info.org/data). For up-to-date information on the study, visit www.ppmi-info.org. PPMI – a public-private partnership – is funded by the Michael J. Fox Foundation for Parkinson's Research and funding partners. A list of the names of all of the PPMI funding partners found at www.ppmi-info.org/fundingpartners.

This work was supported by the National Institute of Biomedical Imaging and Bioengineering (NIBIB) under grant R21 EB016391. The contents are solely the responsibility of the authors and do not necessarily represent the official views of the NIBIB. The authors would also like to thank the nuclear medicine technologists of the UMass Memorial Medical Center who shared their observations regarding patient motion. The DaTscan studies used in this investigation were downloaded from PPMI – a public-private partnership – which is funded by The Michael J. Fox Foundation for Parkinson's Research and funding partners, including Abbott, Biogen Idec, F. Hoffman-La Roche Ltd., GE Healthcare, Genentech and Pfizer Inc. This work was also supported in part by a grant from Philips Healthcare.

VII. REFERENCES

1. Bajaj NH, RA, Grachev ID. Clinical utility of dopamine transporter single photon emission CT (DaT-SPECT) with (I-123) ioflupane in diagnosis of parkinsonian syndromes. J Neurol Neurosurg Psych. 2013; (304436):1–8.
2. Seibyl JP, Marek KL, Quilan D, Sheff K, Zoghbi S, Zea-Ponce Y, Baldwin RM, Fussel B, Smith EO, Charney DS, Hoffer PB, Innis RB. Decreased single-photon emission computed tomographic [123-I] beta-CIT striatal uptake correlates with symptom severity in Parkinson's disease. Ann Neurol. 1995; 38(4):589–598. [PubMed: 7574455]
3. Benamer HTS, Patterson J, Wyper DJ, Hadley DM, Macphee GJA, Grosset DG. Correlation of Parkinson's disease severity and duration with 123-I-FP-CIY SPECT striatal uptake. Movement Disorders. 2000; 15(4):692–698. [PubMed: 10928580]
4. Zubal IG, Early M, Yuan O, Jennings D, Marek KL, Seibyl JP. Optimized, automated striatal uptake analysis applied to SPECT brain scans of Parkinson's disease patients. J Nucl Med. 2007; 48(6): 857–864. [PubMed: 17504864]
5. Dickson JC, Tossici-Bolt L, Sera T, Erlandsson K, Varrone A, Tatsch K, Hutton BF. The impact of reconstruction method on the quantification of DaTSCAN images. Eur J Nucl Med Mol Imaging. 2010; 37(1):23–35. [PubMed: 19618181]
6. Djang DSW, Janssen MJR, Bohnen N, Booij J, Henderson TA, Herholz K, Minoshima S, Rowe CC, Sabri O, Seibyl JP, Van Berckel BNM, Wanner M. SNM practice guideline for dopamine transporter imaging with 123-I-Ioflupane SPECT 1.0. J Nucl Med. 2012; 53(1):154–163. [PubMed: 22159160]
7. Duvall WL, Croft LB, Godiwala T, Ginsberg E, George T, Henzlova JH. Reduced isotope dose with rapid SPECT MPI imaging: Initial experience with a CZT SPECT camera. J Nucl Cardiol. 2010; 17(6):1009–1014. [PubMed: 21069489]
8. Rogulski MM, Barber HB, Barrett HH, Shoemaker RL, Woolfenden J. Ultra-high-resolution brain SPECT imaging: simulation results. IEEE Trans Nucl Sci. 1993; 40:1123–1129.
9. Rowe RKA, JN, Barrett HH, Chen J-C, Klein WP, Moore BA, Pang IW, Patton DD, White TA. A stationary hemispherical SPECT imager for three-dimensional brain imaging. J Nucl Med Tech. 1993; 34(March):474.

10. Furenlid LR, Wilson DW, Chen Y, Kim H, Pietraski PJ, Crawford MJ, Barrett HH. FastSPECTII:A second-generation high-resolution dynamic SPECT Imager. IEEE Trans Nucl Sci. 2004; 51(3): 631–635. [PubMed: 20877439]
11. Goorden MC, Rentmeester MCM, Beekman FJ. Theoretical analysis of full-ring multi-pinhole SPECT. Phys Med Biol. 2009; 54:6593–6610. [PubMed: 19826198]
12. Rentmeester MCM, Van der Have F, Beekman FJ. Optimizing multi-pinhole SPECT geometries using an analytical model. Phys Med Biol. 2007; 52(9):2567–2581. [PubMed: 17440253]
13. Nillius P, Danielsson M. Theoretical bounds and system design for multipinhole SPECT. IEEE Trans Med Imag. 2010; 29(7):1390–1400.
14. Van Audenhaege K, Vandenberghe S, Deprez K, Vandeghinste B, Van Holen R. Design and simulation of a full-ring multi-lofthole collimator for brain SPECT. Phys Med Biol. 2013; 58:6317–6336. [PubMed: 23966017]
15. Jakoby BW, Bercier Y, Conti M, Casey ME, Bendriem B, Townsend DW. Physical and clinical performance of the mCT time-of-flight PET/CT scanner. Phys Med Biol. 2011; 56:2375–2389. [PubMed: 21427485]
16. Moyer RA. A low-energy multihole converging collimator compared with a pinhole collimator. J Nucl Med. 1973; 12(2):59–64.
17. Wooten GF, Currie LJ, Bovbjerg VE, Lee JK, Patrie J. Are men at greater risk for Parkinson's disease than women? J Neurol Neurosurg Psych. 2004; 75(4):637–639.
18. Van Den Eeden SK, Tanner CM, Bernstein AL, Fross RD, Leimpeter A, Bloch DA, Nelson LM. Incidence of Parkinson's Disease: Variation by Age, Gender, and Race/Ethnicity. Amer J Epidem. 2003; 157(11):1015–1022.
19. Mukherjee, JM.; Gifford, H.; King, MA.; Shao, L.; Song, X.; Wang, J. Fast shift-variant resolution compensation within iterative reconstruction for fan-beam collimator. 2009 IEEE Nuclear Science Symposium and Medical Imaging Conference; Orlando. 2009; p. 3230-3234.
20. Mahmood ST, Erlandsson K, Cullum I, Hutton BF. The potential for mixed multiplexed and non-multiplexed data to improve the reconstruction quality of a multi-slit-slat collimator SPECT system. Phys Med Biol. 2010; 55:2247–2268. [PubMed: 20354282]
21. Mok GSP, Tsui BMW, Beekman FJ. The efects of object activity distributions on multiplexing multi-pinhole SPECT. Phys Med Biol. 2011; 56:2635–2650. [PubMed: 21454926]
22. Lin J. On artifact-free projection overlaps in multi-pinhole tomographic imaging. IEEE Trans Med Imaging. 2013; 32:2215–2229.
23. Van Audenhaege K, Vanhove C, Vandenberghe S, Van Holen R. The evaluation of data completeness and image quality in multiplexing multi-pinhole SPECT. IEEE Trans Med Imaging. 2015; 34(2):474–486. [PubMed: 25291791]
24. Deprez, K.; Van Holen, R.; Vandenberghe, S. The lofthole: a novel shaped pinhole geometry for optimal detector usage without multiplexing and without addditional shielding. Proceedings of 2011 IEEE Nuclear Science Symposium and Medical Imaging Conference; 2011. p. 3317-3322.
25. Deprez K, Pato L, Van Holen R, Vandenberghe S. Characterization of a SPECT pinhole collimator for optimal detector usage (the lofthole). Phys Med Biol. 2013; 58(4):859–885. [PubMed: 23337658]
26. Williams MB, Stolin AV, Kundu BK. Investigation of efficiency and spatial resolution using pinholes with small pinhole angle. IEEE Trans Nucl Sci. 2003; 50(5):1562–1568.
27. Xia, D.; Park, M-A.; Moore, SC.; Metzler, SD. Preliminary Investigation of Imaging Properties for Sub-Millimeter Square-Pinholes. 2013 IEEE Nuclear Science Symposium and Medical Imaging Conference; 2013.
28. Poston, A. DOD. Human Engineering Design Data Digest. 2000.
29. Metzler SD, Accorsi R, Novak JR, Ayan AS, Jaszczak RJ. On-axis sensitivity and resolution of a slit-slat collimator. J Nucl Med. 2006; 47(11):1884–1890. [PubMed: 17079823]
30. Weber, DA.; Eckerman, KF.; Dillman, LT.; Ryman, JC. MIRD: Radionuclide Data and Decay Schemes. Society of Nuclear Medicine; 1989.
31. Lee TC, Ellin JR, Huang Q, Shrestha U, Gullberg GT, Seo Y. Multipinhole collimator with 20 apertures for a brain SPECT application. Med Phys. 2014; 41(11):112501-1-7. [PubMed: 25370660]

32. Aguiar P, Pino F, Sliva-Rodriguez J, Pavia J, Ros D, Ruibal A, El Bitar Z. Analytical, experimental, and Monte Carlo system response matrix for pinhole SPECT reconstruction. Med Phys. 2014; 41(3):032501-1-10. [PubMed: 24593739]

33. Hoffman EJ, Huang G, Phelps ME. Quantitation in positron emission computed tomography: 1. Effect of object size. J Comput Assist Tomogr. 1979; 3:299–308. [PubMed: 438372]

34. Kessler RM, Ellis JR Jr, Eden M. Analysis of emission tomographic scan data: limitations imposed by resolution and background. J Comput Assist Tomogr. Jun; 1984 8(3):514–522. [PubMed: 6609942]

35. Muehllehner G. Effect of resolution improvement on required count density in ECT imaging: a computer simulation. Phys Med Biol. Feb; 1985 30(2):163–173. [PubMed: 3872464]

36. Mueller SP, Polak JF, Kijewski MF, Holman BL. Collimator selection for SPECT brain imaging: the advantage of high resolution. J Nucl Med. Nov; 1986 27(11):1729–1738. [PubMed: 3021935]

37. Park MA, Moore SC, Kijewski MF. Brain SPECT with short focal-length cone-beam collimator. Med Phys. 2005; 32(7):2236–2244. [PubMed: 16121578]

38. Metzler SD, Accorsi R. Resolution- versus sensitivity -effective diameter in pinhole collimation:experimental verfications. Phys Med Biol. 2005; 50:5005–5017. [PubMed: 16237237]

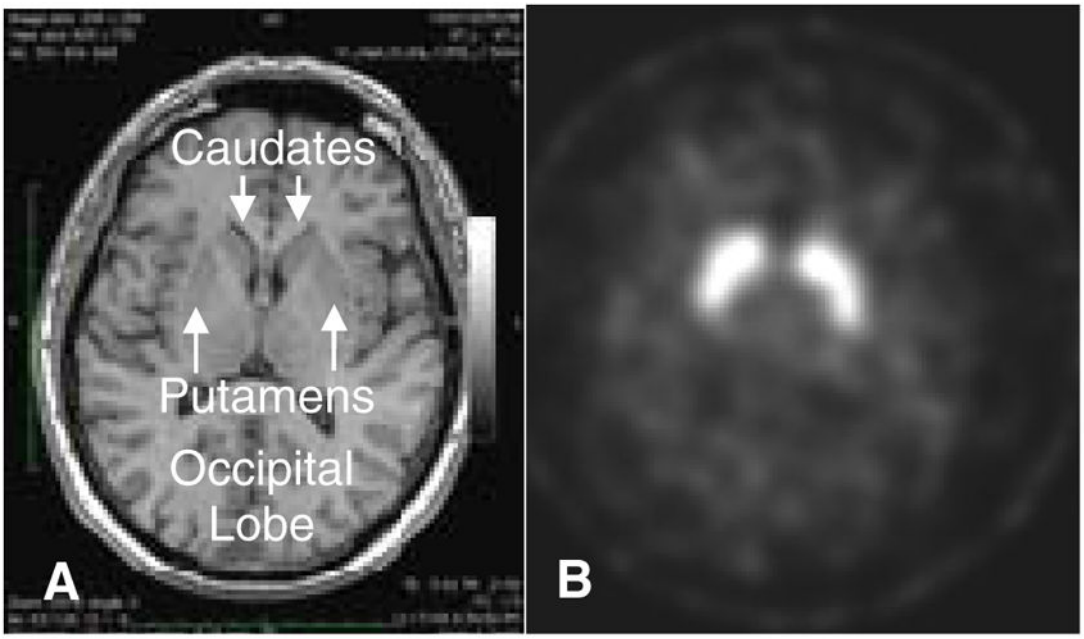

Figure 1.

A. Transverse MRI slice with putamen, caudate, and region of occipital lobe labeled (source: John Seibyl MD, Molecular NeuroImaging LLC). B. Transverse slices of I-123 DaTScan through putamen and caudate acquired on a Philips Prism3000 with low-energy high-resolution (LEHR) fan –beam collimators. Note putamen and caudate visually are not separated.

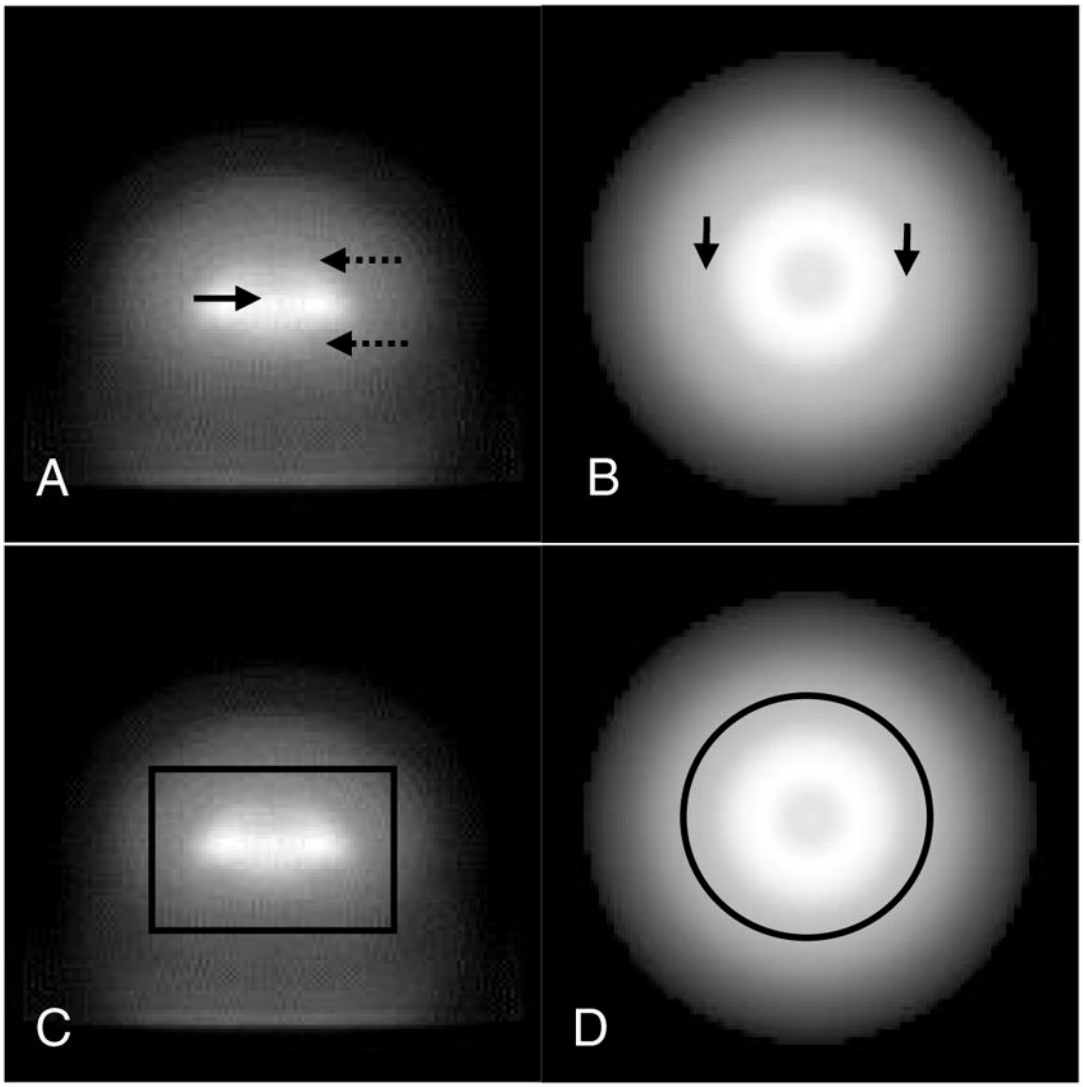

Figure 2.

Determination of volume of interest (VOI) for MPH collimator design using an I-123 DaTscan study acquired on a Prism3000 with fan-beam collimators. A. Illustration of the interactive determination of the axial location of the center (pointed to by solid black arrow) and extent (pointed to by the two dashed arrows) of the striatal distribution on the parallel reprojection of the attenuation corrected transverse slices summed over 360°. B. Determination of the lateral extent of the region of striatal localization is illustrated by the locations of the two arrows on the display of the sum of all the transverse slices that was in turn summed for rotation over 360°. C. Visualization of the height and width of the 12.0 by 8.0 cm VOI shown as the black rectangle superimposed on the image of A. Note how well this encompasses the striatal region of this patient. D. Cross-sectional view of the VOI (black circle) superimposed on the summed and rotated transverse slices of a patient study as shown in B. Again note how well the striatal activity distribution fits within the VOI.

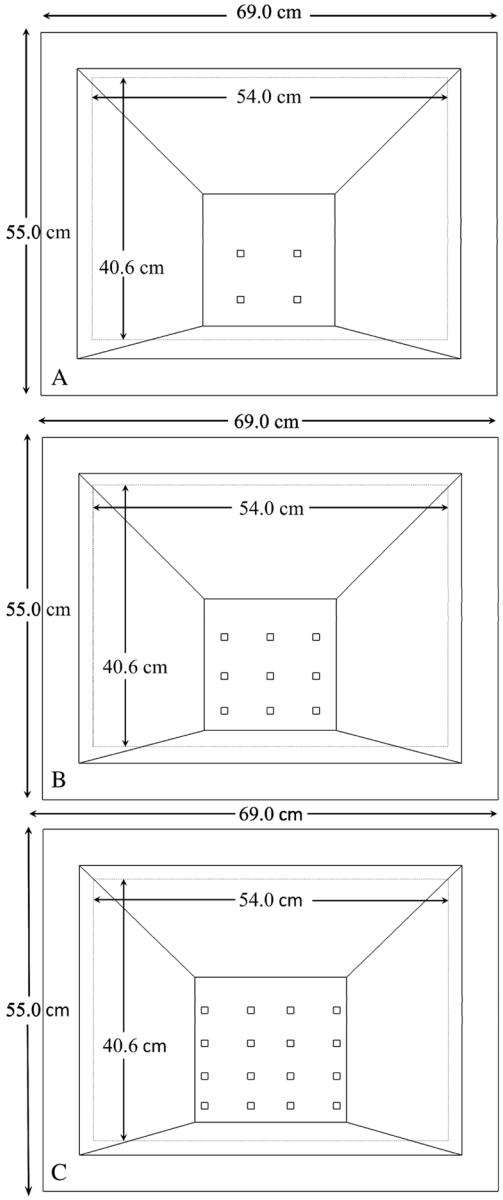

Figure 3.

Frontal view of MPH collimators for aperture arrays of: A. 2 × 2, B. 3 × 3, and C. 4 × 4 pinholes. The 54 by 40.6 surface of the NaI(Tl) crystal beneath the MPH collimator is shown by the gray rectangle.

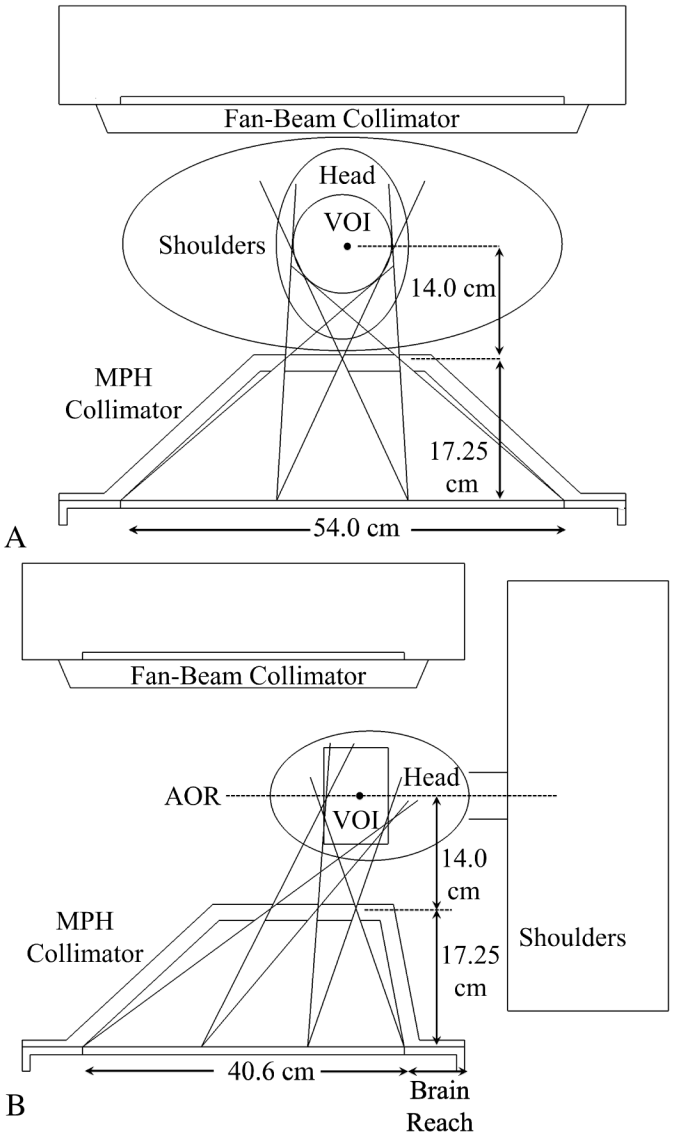

Figure 4.

A. Side view for caudal row of apertures of 3 × 3 MPH collimator showing 12.0 cm diameter VOI, focal point at the center of VOI, geometrical viewing limits for each aperture and elliptical outlines depicting the head and shoulders. Also shown are the fan-beam collimator and camera head. B. top view of center row of apertures of 3 × 3 MPH collimator showing AOR, 12.0 × 8.0 cm diameter VOI, and geometrical viewing limits for each aperture relative to the VOI. Also shown are the fan-beam collimator and its camera head, and the brain reach is indicated.

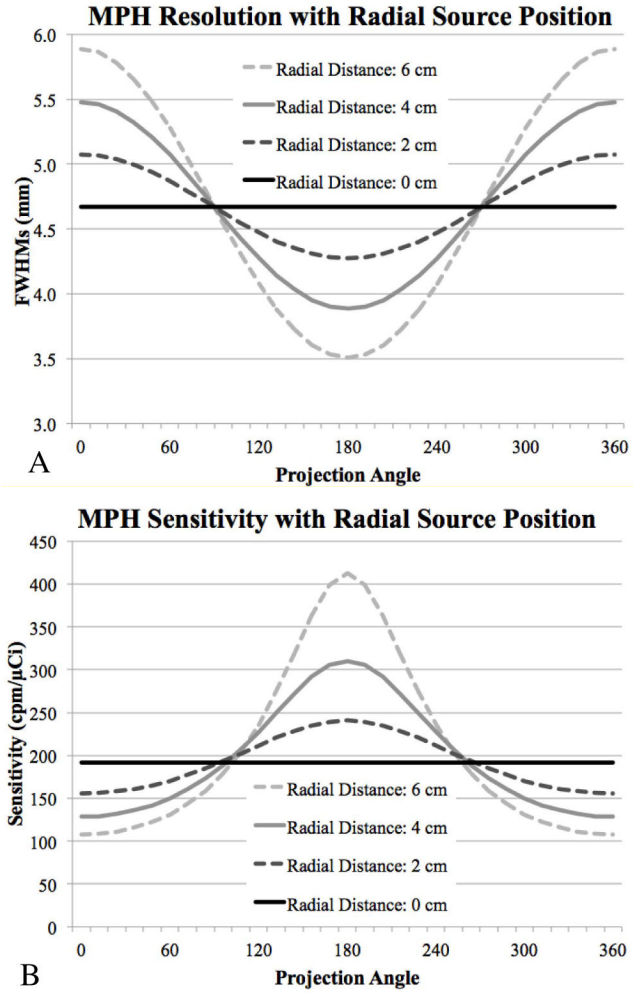

Figure 5.

Shown in A. is variation in system spatial resolution ($FWHM_S$) and in B. is variation in sensitivity with projection angle as a function of radial displacement from the center of the VOI for the 3 × 3 array MPH collimator.

Table I

Comparison of Parameters and Sensitivities of MPH Collimator Arrays

Collimator	Aperture to Detector (cm)	Average Hole Size d (mm)	g (cpm/μCi)
2 × 2	20.0	2.6	127
3 × 3	17.25	2.2	192
4 × 4	13.0	1.6	159

Table II

Comparison of System Spatial Resolution and Geometric Sensitivity for the 3 × 3 Array MPH and Fan-Beam Collimators

Collimator	$FWHM_S$ (mm)	g (cpm/μCi)
MPH	4.7	192
LEHR-Fan	8.9	312
LEUHR-Fan	7.4	191
LEHR-Parallel	9.2	228
LEUHR-Parallel	7.6	139

Table III

Comparison of Average System Spatial Resolution and Geometric Sensitivity for the 3 × 3 Array MPH Collimator with Radial Displacement

Position	$FWHM_S$ (mm)	g (cpm/μCi)
Center	4.7	192
2 cm	4.6	197
4 cm	4.6	206
6 cm	4.6	219